

## Solvophobic Acceleration of Diels–Alder Reactions in Supercritical Carbon Dioxide

Jin Qian,<sup>†,‡</sup> Michael T. Timko,<sup>†</sup> Andrew J. Allen,<sup>†</sup> Christopher J. Russell,<sup>†</sup> Bozena Winnik,<sup>§</sup> Brian Buckley,<sup>§</sup> Jeffrey I. Steinfeld,<sup>†,‡</sup> and Jefferson W. Tester<sup>\*,†,‡</sup>

*Contribution from the Departments of Chemistry and Chemical Engineering and the Laboratory for Energy and the Environment, Massachusetts Institute of Technology, Cambridge, Massachusetts 02139 and Environmental and Occupational Health Sciences Institute, Rutgers University, Piscataway, New Jersey 08854*

Received November 10, 2003; E-mail: testerel@mit.edu

**Abstract:** The rate of the Diels–Alder reaction between *N*-ethylmaleimide and 9-hydroxymethylanthracene in supercritical carbon dioxide (scCO<sub>2</sub>) was determined by following the disappearance of 9-hydroxymethylanthracene with in situ UV/vis absorption spectroscopy. The reaction conditions were 45–75 °C and 90–190 bar, which correspond to fluid densities (based on pure carbon dioxide) ranging between approximately 340 and 730 kg m<sup>-3</sup>. The measured reaction rate at low scCO<sub>2</sub> fluid densities was nearly 25× faster than that reported in acetonitrile at the same temperature (45 °C). An inverse relationship between reaction rate and fluid density/pressure was observed at all temperatures in scCO<sub>2</sub>. The apparent activation volumes were large and positive (350 cm<sup>3</sup> mol<sup>-1</sup>) and only a weak function of reduced temperature. A solvophobic mechanism analogous to those observed in conventional solvents is postulated to describe (a) the rate acceleration observed for this reaction in scCO<sub>2</sub> relative to that in acetonitrile, (b) the observed relationship between reaction rate and pressure/temperature/density, and (c) the large, positive activation volumes. Solubility measurements in scCO<sub>2</sub>, rate measurements in conventional solvents, and an empirical correlation are used to support this theory. Our results advance the general understanding of reactivity in supercritical fluids and provide a rationale for selecting reactions which can be accelerated when conducted in scCO<sub>2</sub>.

### Introduction

The need for replacement solvents as reaction media for chemical synthesis has been clear for some time due to concerns surrounding the potential environmental and health risks of many traditional hydrocarbon solvents. For example, benzene, methylene chloride, and chloroform are being phased out as a result of U.S. FDA and U.S. EPA regulations to limit industrial emissions.<sup>1,2</sup> Due to its high density at moderate conditions ( $\rho_c = 0.466 \text{ g cm}^{-3}$ ,  $T_c = 31.1 \text{ °C}$ ,  $P_c = 73.8 \text{ bar}$ ), nontoxicity, and nonflammability, near-critical and supercritical carbon dioxide (scCO<sub>2</sub>) is a promising solvent for organic synthesis. Ongoing research efforts into the use of scCO<sub>2</sub> as an environmentally friendly or “green” solvent are well documented.<sup>3–6</sup>

The study of model reactions is an efficient way to improve understanding of chemical reactivity in scCO<sub>2</sub>. The Diels–Alder cycloaddition is a well-defined bimolecular reaction that is an excellent model for the purposes of developing green solvents. Furthermore, the Diels–Alder reaction is one of the most important synthetic reactions for the construction of six-membered rings and has been the subject of numerous studies in scCO<sub>2</sub><sup>7–20</sup> and subcritical<sup>9,20</sup> and supercritical<sup>21</sup> propane. With the exception of one published report,<sup>8</sup> the rates of Diels–Alder

<sup>†</sup> Departments of Chemistry and Chemical Engineering, Massachusetts Institute of Technology.

<sup>‡</sup> Laboratory for Energy and the Environment, Massachusetts Institute of Technology.

<sup>§</sup> Rutgers University.

- (1) *Green Chemistry: Challenging Perspectives*; Tundo, P., Anastas, P. T., Eds.; Oxford University Press: New York, 2000.
- (2) *Green Chemistry: Theory and Practice*; Anastas, P. T., Warner, J. C., Eds.; Oxford University Press: New York, 1998.
- (3) *Chemical Synthesis Using Supercritical Fluids*; Jessop, P. G., Leitner, W., Eds.; Wiley-VCH: New York, 1999.
- (4) Tester, J. W.; Danheiser, R. L.; Weinstein, R. D.; Renslo, A.; Taylor, J. D.; Steinfeld, J. I. *ACS Symp. Ser.* **2000**, 767, 270.
- (5) Oakes, R. S.; Clifford, A. A.; Rayner, C. M. *J. Chem. Soc., Perkins Trans. I* **2001**, 9, 917.
- (6) Leitner, W. *Acc. Chem. Res.* **2002**, 35, 746.

- (7) Glebov, E. M.; Krishtopa, L. G.; Stepanov, V.; Krasnoperov, L. N. *J. Phys. Chem. A* **2001**, 105, 9427.
- (8) Thompson, R. L.; Gläser, R.; Bush, D.; Liotta, C. L.; Eckert, C. A. *Ind. Eng. Chem. Res.* **1999**, 38, 4220.
- (9) Reaves, J. T.; Roberts, C. B. *Chem. Eng. Commun.* **1999**, 171, 117.
- (10) Lin, B.; Akgerman, A. *Ind. Eng. Chem. Res.* **1999**, 38, 4525.
- (11) Ikushima, Y.; Pople, K.; Gaskill, W. J.; Bartle, K. D.; Rayner, C. M. *J. Chem. Soc., Faraday Trans.* **1998**, 94, 1451.
- (12) Renslo, A. R.; Weinstein, R. D.; Tester, J. W.; Danheiser, R. L. *J. Org. Chem.* **1997**, 62, 4530.
- (13) Clifford, A. A.; Pople, K.; Gaskill, W. J.; Bartle, K. D.; Rayner, C. M. *Chem. Commun.* **1997**, 6, 595.
- (14) Weinstein, R. D.; Renslo, A. R.; Danheiser, R. L.; Harris, J. G.; Tester, J. W. *J. Phys. Chem.* **1996**, 100, 12337.
- (15) Ikushima, Y.; Saito, N.; Sato, O.; Arai, M. *Bull. Chem. Soc. Jpn.* **1994**, 67, 1734.
- (16) Ikushima, Y.; Ito, S.; Asanao, T.; Yokoyama, T.; Saito, N.; Hatakeda, K.; Goto, T. *J. Chem. Eng. Jpn.* **1990**, 23, 96.
- (17) Kim, S.; Johnston, K. P. *Chem. Eng. Commun.* **1988**, 63, 49.
- (18) Paulaitis, M. E.; Alexander, G. C. *Pure Appl. Chem.* **1987**, 59, 61.
- (19) Isaacs, N. S.; Keating, N. J. *Chem. Soc., Chem. Commun.* **1992**, 12, 876.
- (20) Reaves, J. T.; Roberts, C. B. *Ind. Eng. Chem. Res.* **1999**, 38, 855.
- (21) Knutson, B. L.; Dillow, B. L.; Liotta, A. K.; Liotta, C. L.; Eckert, C. A. *ACS Symp. Ser.* **1995**, 608, 166.

reactions in scCO<sub>2</sub> are generally somewhat slower than those observed in hydrocarbon solvents. Also, most studies indicate that increasing the fluid density/pressure increases the observed reaction rate, with exceptions<sup>8,10</sup> having been observed in the vicinity of the mixture critical point. Selectivities<sup>11–13,17</sup> of Diels–Alder reactions in scCO<sub>2</sub> are comparable to those observed in hydrocarbon solvents.

The high pressures required for supercritical fluid processing are a major obstacle to its industrial use. To have an impact on industrial practice, it will be necessary to demonstrate significant technological and environmental advantages for using scCO<sub>2</sub> as a reaction solvent. Efforts to demonstrate such technological advantages have focused on exploiting the physicochemical properties of scCO<sub>2</sub>. For instance, its favorable transport properties<sup>3,22</sup> have been used to improve reaction rates, selectivities, and catalyst lifetimes for heterogeneously catalyzed transformations.<sup>23,24</sup> The high solubility of carbon dioxide in polymers has been used to increase reactant accessibility to encapsulated<sup>25</sup> catalysts and to facilitate solid-phase polymerizations.<sup>26</sup> The high solubility of gases such as H<sub>2</sub> and CO in scCO<sub>2</sub> has been exploited in a number of reactions including hydrogenations<sup>27,28</sup> and hydroformylations,<sup>29–32</sup> sometimes with substantially improved regioselectivities compared to those of conventional solvents.<sup>32</sup> Carbon dioxide, at conditions near or above its critical point, has also been used as a reactant<sup>33–35</sup> and reversible protecting group.<sup>36</sup> Comparatively less emphasis has been placed on the molecular-level analysis of solvation effects of scCO<sub>2</sub> on chemical kinetics. Many of the important technological advantages of scCO<sub>2</sub> as a reaction solvent have been demonstrated for catalyzed systems<sup>6,27–36</sup> which proceed via complex mechanisms, making their molecular-level interpretation rather difficult. Previous attempts to predict or correlate trends for elementary reactions such as the Diels–Alder cycloaddition have relied upon thermodynamic<sup>8,9,11,13,21</sup> or kinetic<sup>14</sup> fitted parameters without the benefit of molecular-level analysis.

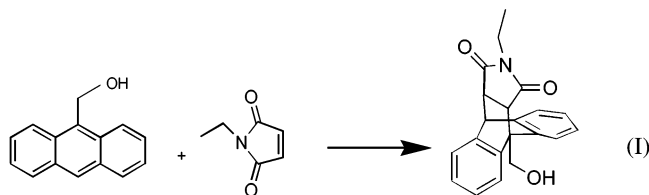
Our approach was to draw upon the considerable knowledge base developed for Diels–Alder reactions in incompressible solvents (e.g., hydrocarbons, fluorocarbons, water) to gain insight regarding molecular-level solvation effects in a supercritical fluid. Our analysis was based primarily on studies which investigated the use of aqueous and fluorinated solvents.

Following the pioneering work of Breslow<sup>37,38</sup> and Grieco<sup>39</sup> in the early 1980s, it is now well established that the rates and sometimes selectivities of certain Diels–Alder reactions are dramatically improved when they are conducted in aqueous rather than hydrocarbon solvents. It is generally agreed that solvophobic interactions and an enhanced hydrogen-bonding effect, which preferentially stabilizes the polarized transition state, are the main contributors to this rate enhancement.<sup>40–42</sup> Current research efforts in this area have focused on quantifying the relative energetic contributions of these two effects for a given set of reagents.<sup>42</sup>

More recently, it was reported that fluorinated media also accelerate certain organic reactions including Diels–Alder cycloadditions,<sup>43,44</sup> conjugate additions of amines,<sup>44</sup> and esterification of acids and alcohols.<sup>45</sup> The most striking example is the 50-fold acceleration of the Diels–Alder reaction of 9-hydroxymethylanthracene (diene) and *N*-ethylmaleimide (dienophile) when carried out in perfluorohexane rather than acetonitrile.<sup>43</sup> It is hypothesized that the origin of the acceleration in fluorinated solvents is entirely solvophobic, since the solvents which have been studied thus far lack the capacity to form hydrogen bonds.

Observations of rate and selectivity improvements in aqueous and fluorinated solvents are directly relevant to chemical reactivity in supercritical fluids. Specifically, because scCO<sub>2</sub> and fluorinated compounds behave similarly as solvents, accelerative mechanisms observed in one might also be operative in the other. If such an analogy holds, then the considerable literature of Diels–Alder reactivity in conventional solvents could be used to interpret observations made in supercritical systems and to form a basis for selection of model reactions.

The objectives of this theoretical study are (1) to demonstrate that the model Diels–Alder cycloaddition of 9-hydroxymethylanthracene and *N*-ethylmaleimide (reaction I) shows dramatic rate accelerations in scCO<sub>2</sub> and (2) to understand the mechanism(s) responsible for this acceleration.



- (22) *Supercritical Fluid Extraction*, 2nd ed.; McHugh, M. A., Krukoni, V. J., Eds.; Butterworth-Heinemann: Boston, 1994.
- (23) Baiker, A. *Chem. Rev.* **1999**, *99*, 453.
- (24) Subramaniam, B.; Lyon, C. J.; Arunajatesan, V. *Appl. Catal., B* **2002**, *37*, 279.
- (25) Ley, S. V.; Ramarao, C.; Gordon, R. S.; Holmes, A. B.; Morrison, A. J.; McConvey, I. F.; Shirley, I. M.; Smith, S. C. *Chem. Commun.* **2002**, 1134.
- (26) (a) Shi, C. M.; DeSimone, J. M.; Kiserow, D. J.; Roberts, G. W. *Macromolecules* **2001**, *34*, 7744. (b) Gross, S. M.; Roberts, G. W.; Kiserow, D. J.; DeSimone, J. M. *Macromolecules* **2000**, *33*, 40. (c) Gross, S. M.; Flowers, D.; Roberts, G.; Kiserow, D. J.; DeSimone, J. M. *Macromolecules* **1999**, *32*, 3167.
- (27) Burk, M. J.; Feng, S.; Gross, M. F.; Tumas, W. *J. Am. Chem. Soc.* **1995**, *117*, 8277.
- (28) Goetheer, E. L. V.; Verkerk, A. W.; van den Broeke, L. J. P.; de Wolf, E.; Deelman, B.-J.; van Koten, G.; Keurentjes, J. T. F. *J. Catal.* **2003**, *219*, 126.
- (29) (a) Davis, T.; Erkey, C. *Ind. Eng. Chem. Res.* **2000**, *39*, 3671. (b) Palo, D. R.; Erkey, C. *Organometallics* **2000**, *19*, 81. (c) Palo, D. R.; Erkey, C. *Ind. Eng. Chem. Res.* **1999**, *38*, 3786. (d) Palo, D. R.; Erkey, C. *Ind. Eng. Chem. Res.* **1999**, *38*, 2163. (e) Palo, D. R.; Erkey, C. *Ind. Eng. Chem. Res.* **1998**, *37*, 4203.
- (30) (a) Lopez-Castillo, Z. K.; Flores, R.; Kani, I.; Fackler, J. P.; Akgerman, A. *Ind. Eng. Chem. Res.* **2003**, *42*, 3893. (b) Lin, B.; Akgerman, A. *Ind. Eng. Chem. Res.* **2001**, *40*, 1113.
- (31) Mechan, N. J.; Sandee, A. J.; Reek, J. N. H.; Kamer, P. C. J.; van Leeuwen, P. W. N. M.; Poliakoff, M. *Chem. Commun.* **2000**, 1497.
- (32) Koch, D.; Leitner, W. *J. Am. Chem. Soc.* **1998**, *120*, 13398.
- (33) (a) Jessop, P. G.; Hsiao, Y.; Ikariya, T.; Noyori, R. *J. Am. Chem. Soc.* **1996**, *118*, 344. (b) Jessop, P. G.; Ikariya, T.; Noyori, R. *Chem. Rev.* **1995**, *95*, 259. (c) Jessop, P. G.; Hsiao, Y.; Ikariya, T.; Noyori, R. *J. Am. Chem. Soc.* **1994**, *116*, 8851. (d) Jessop, P. G.; Ikariya, T.; Noyori, R. *Nature* **1994**, *368*, 231.
- (34) Schmid, L.; Schneider, M. S.; Engel, D.; Baiker, A. *Catal. Lett.* **2003**, *88*, 105.
- (35) Isaacs, N. S.; O'Sullivan, B.; Verhaelen, C. *Tetrahedron* **1999**, *55*, 11949.

- (36) Wittmann, K.; Wisniewski, W.; Mynott, R.; Leitner, W.; Kranemann, C. L.; Rische, T.; Eilbracht, P.; Kluwer, S.; Ernsting, J. M.; Elsevier, C. *Chem.—Eur. J.* **2001**, *7*, 4584.
- (37) Rideout, D. C.; Breslow, R. *J. Am. Chem. Soc.* **1980**, *102*, 7816.
- (38) Breslow, R.; Maitra, U. *Tetrahedron Lett.* **1984**, *25*, 1239.
- (39) Grieco, P. A.; Garner, P.; He, Z. *Tetrahedron Lett.* **1983**, *24*, 1897.
- (40) Otto, S.; Blokzijl, W.; Engberts, J. B. F. N. *J. Org. Chem.* **1994**, *59*, 5372.
- (41) Otto, S.; Engberts, J. B. F. N. *Pure Appl. Chem.* **2000**, *72*, 1365.
- (42) Chandrasekhar, J.; Shariffskul, S.; Jorgensen, W. L. *J. Phys. Chem. B* **2002**, *106*, 8078.
- (43) Myers, K. E.; Kumar, K. *J. Am. Chem. Soc.* **2000**, *122*, 12025.
- (44) Jenner, G.; Gacem, B. *J. Phys. Org. Chem.* **2003**, *16*, 265.
- (45) Gacem, B.; Jenner, G. *Tetrahedron Lett.* **2003**, *44*, 1391.

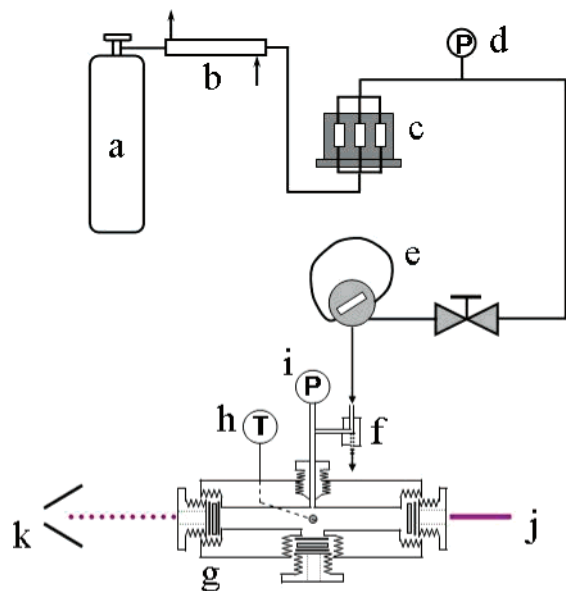


**Figure 1.** Simplified schematic of the high-pressure system used to obtain kinetic data in this study. Depicted are the (a) cylinder of grade 5.5 CO<sub>2</sub>, (b) heat exchanger to liquefy the gaseous CO<sub>2</sub>, (c) high-pressure pump (Eldex, BBB-4) for delivering liquid CO<sub>2</sub> at high pressures to the reactor, (d) digital pressure transducer (Dynisco) for measuring system pressure, (e) HPLC valve (Valco Instruments, uw-type), (f) three-way valve which served as the reactor inlet and outlet, (g) high-pressure reactor equipped with an  $\alpha$ -Al<sub>2</sub>O<sub>3</sub> sapphire window for either transmission or scattering spectroscopy, (h) T-type thermocouple for measuring fluid temperature, (i) analog pressure gauge (Matheson, 63-3133) for measuring pressure within the reactor, (j) source of monochromatic UV radiation, and (k) spectrophotometer detector.

## Experimental Section

**Reagents.** 9-Hydroxymethylanthracene, *N*-ethylmaleimide, and all solvents (HPLC-grade) were obtained from Sigma Aldrich and used without further purification. Grade 5.5 carbon dioxide (>99.99%) was purchased from BOC and used as received. Water was deionized to a minimum resistivity of 18.1 M $\Omega$  cm using a Barnstead Nanopure filtration system.

**Kinetic Measurements.** The simplified experimental schematic is shown in Figure 1. Reactions were performed in a 316-stainless-steel, high-pressure, temperature-controlled reactor which was insulated externally with fiberglass tape. The optically accessible reactor used in this study was designed in our research group.<sup>46</sup> The reactor was cylindrical with a working volume of approximately 3 cm<sup>3</sup>. Sapphire ( $\alpha$ -Al<sub>2</sub>O<sub>3</sub>) windows were positioned at opposing ends of the reactor (path length of 2.9 cm) and were used for optical access and absorption spectroscopy. Although the reaction mixture could be agitated using a standard Teflon-coated stir bar, practically, it was found that the stir bar interfered with spectroscopic measurements. Therefore, the stir bar was used only in select experiments to confirm that diffusion and free convection alone were sufficient for good mixing over the time scales of experimental interest. Temperature was monitored to within  $\pm 0.5$  °C with a T-type thermocouple inserted into the fluid and maintained using a combination of a PID controller (Omega, 9001CN) and thermal tape (Barnstead). Pressure was measured to within  $\pm 1$  bar using a standard Bourdon-tube pressure gauge (Matheson, 63-3133).

Reactions were initiated by injection of a solution of *N*-ethylmaleimide and 9-hydroxymethylanthracene in either acetonitrile or acetone solution into the reactor through an HPLC valve (Valco Instruments Co. Inc., uw-type) using pressurized CO<sub>2</sub>. The solution injection method was used because the reagents are both solids at room temperature and

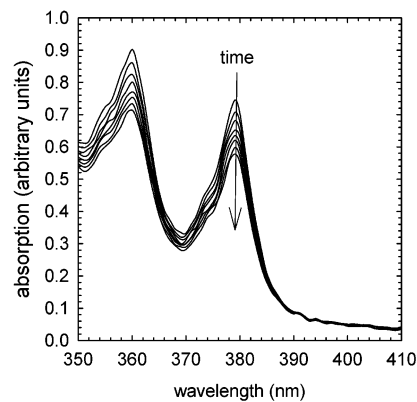


**Figure 2.** Disappearance of the 379 nm peak of 9-hydroxymethylanthracene in scCO<sub>2</sub> during the course of a reaction. Conditions: 45 °C, 101 bar ( $\rho = 518$  kg m<sup>-3</sup>). Spectra for the first 4 h of a 16 h long run are shown.

dissolved slowly into scCO<sub>2</sub>. For the majority of the experiments, the initial concentrations of 9-hydroxymethylanthracene and *N*-ethylmaleimide were 0.02 mol L<sup>-1</sup> ( $2.2 \times 10^{-6}$  mole fraction at a fluid density of 0.4 g cm<sup>-3</sup>) and  $1 \times 10^{-3}$  mol L<sup>-1</sup> ( $1.0 \times 10^{-4}$  mole fraction at a fluid density of 0.4 g cm<sup>-3</sup>), respectively. The ratio of dienophile to diene was varied, but was always greater than 50:1 (in molar units) to ensure pseudo-first-order kinetics. The mole percentage of the cosolvent was always less than 3.5% but was approximately 0.2% in most experiments. Changing neither the cosolvent (either acetone or acetonitrile) nor its concentration had an effect on the measured reaction rate within the limits of experimental reproducibility ( $\pm 5\%$ ).

Although visual inspection of the reaction mixtures indicated one-phase behavior for all experiments, the presence of a small volume of a second phase is sometimes difficult to confirm visually. Variation of the initial concentrations of the two reagents served to confirm that, if an undetected second phase were present, it did not appreciably affect kinetic rate measurements. The reaction temperature was varied from 45 to 75 °C, and pressure was varied from 90 to 190 bar. These conditions correspond to a density range of 340–730 kg m<sup>-3</sup> as calculated by an accurate<sup>47</sup> equation of state (EOS) assuming that the reaction mixture could be treated as pure carbon dioxide. Given the dilute concentrations of reactants and injection solvent used in this study, the error introduced by treating the reaction mixture as pure carbon dioxide is minimal.

The rate of reaction I was measured by in situ monitoring of the disappearance of the absorption peak of 9-hydroxymethylanthracene at 379 nm (at which wavelength interference from the sapphire windows and other species in the reaction mixture was negligible) using a Varian Cary 50 UV/vis spectrophotometer. The reaction progress was monitored for roughly 18 h (i.e., 1–4 reaction half-lives depending on the conditions). Spectra from a representative run are presented in Figure 2. First-order plots of the logarithm of 9-hydroxymethylanthracene disappearance over time were always linear with little scatter as depicted for several representative runs in Figure 3. Uncertainties in the slopes of these plots were always less than  $\pm 4\%$ . The second-order rate constant was calculated by dividing the slope of the assumed first-order plot by the concentration of excess dienophile, which was known to within  $\pm 2\%$  on the basis of its postreaction recovery. Control experiments, in which only one of the two reagents was injected, indicated that the compounds were stable indefinitely in the reaction vessel and did not adsorb appreciably to the reactor walls; drift in the 379 nm absorption peak of 9-hydroxymethylanthracene was less than  $\pm 2\%$ . On the basis of these three sources of uncertainty (scatter in the pseudo-first-order plots, reactant adsorption, and uncertainty in the concentration of excess dienophile), the error in measured rate constants was estimated to be less than  $\pm 10\%$ .

(46) Taylor, J. D. Ph.D. Thesis, Massachusetts Institute of Technology, Cambridge, MA, 2001.

(47) Span R.; Wagner, W. *J. Phys. Chem. Ref. Data* **1996**, *25*, 1509.

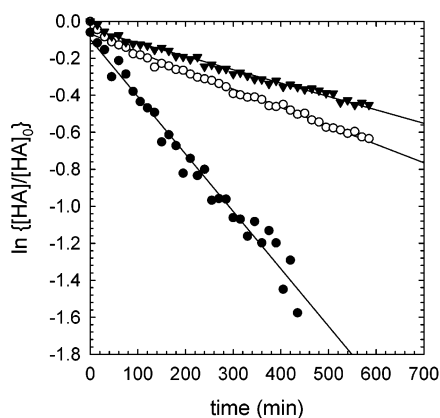


**Figure 3.** Representative first-order plots for reaction I obtained at 60 °C in scCO<sub>2</sub> at various pressures: ▼, 178 bar; ○, 161 bar; ●, 115 bar. [HA] is the instantaneous concentration of 9-hydroxymethylanthracene, and [HA]<sub>0</sub> is its initial concentration. Solid lines are the best fits for the data. The slopes were used to calculate the true second-order rate constant using the known concentration of excess dienophile.

**Analytical Methods.** The adduct in the reaction was identified offline by reversed-phase high-performance liquid chromatography (HPLC; Waters 2690) with tandem mass spectroscopic (MS/MS; LCQ, Finnigan) detection utilizing an atmospheric pressure chemical ionization interface. A Zorbax SB-C18 column (4.6 mm × 15 cm) was used with flash column chromatography (25% ethyl acetate/hexanes). A sample volume of 50 μL was injected for each analysis. The composition of the binary isocratic mobile phase was 0.499 acetonitrile/0.499 water/0.002 formic acid. Operating parameters of the MS/MS system were first auto-optimized in full scan mode and then manually adjusted by flow injection analysis of each target compound at a concentration of 1 mg L<sup>-1</sup>. Target compounds were identified in both full scan mode and selected ion monitoring (SIM) mode by infusion by matching the retention times and mass spectra with standards. The adduct was synthesized by refluxing *N*-ethylmaleimide and 9-hydroxymethylanthracene in a 9:1 CHCl<sub>3</sub>/CH<sub>3</sub>OH solution for 24 h.

For several representative kinetic runs conducted in scCO<sub>2</sub>, the reactor contents were collected by depressurizing the reaction mixture through cold acetonitrile. These postreaction mixtures were analyzed using the HPLC–MS/MS technique, which indicated that mass balance closure of the diene was greater than 85% and that the only product was the Diels–Alder adduct of reaction I. Further analytical details are available in the Supporting Information.

**Solubility Measurements.** Measurements of the solubility of 9-hydroxymethylanthracene in scCO<sub>2</sub> at 45 °C and 70–150 bar were performed by measuring the UV absorbance (at 379 nm using the Varian spectrophotometer) of samples withdrawn from the reactor. Around 4 mg of solid 9-hydroxymethylanthracene was loaded into a 25 mL high-pressure view cell which has been described previously in the literature.<sup>12</sup> At each pressure, the supercritical solution was stirred vigorously for 1 h and allowed to settle, unstirred, for 2 h prior to sample collection. A fraction of the mixture (between 10 and 50 μL) was withdrawn through an HPLC valve (Valco Instruments, uw-type) and then slowly discharged into cold solvent. The precipitated 9-hydroxymethylanthracene was washed from the loop with additional cold solvent and diluted to a standard volume prior to spectroscopic analysis.

**Kinetic Measurements at Atmospheric Pressure.** The rate of the Diels–Alder reaction of *N*-ethylmaleimide with 9-hydroxymethylanthracene was measured at atmospheric pressure in water and acetonitrile over the temperature range 20–50 °C. An Agilent 8532 spectrophotometer equipped with an internal stirring motor and a Peltier heater was used for the measurements. A 100-fold excess of dienophile was used in all experiments, and the initial concentration of 9-hydroxymethylanthracene was 1 × 10<sup>-3</sup> mol L<sup>-1</sup> for experiments conducted in acetonitrile and 2 × 10<sup>-5</sup> mol L<sup>-1</sup> for experiments conducted in water.

**Table 1.** Rate Constants,  $k_c$ , Measured in This Study for the Reaction of 9-Hydroxyanthracene and *N*-Ethylmaleimide in scCO<sub>2</sub><sup>a</sup>

run no.	$k_c$ (10 <sup>3</sup> L mol <sup>-1</sup> s <sup>-1</sup> )	$T$ (°C)	$P$ (bar)	$\rho$ (kg m <sup>-3</sup> )
1	25	45	90	340 ± 20
2	23	45	93	380 ± 30
3	21	45	97	440 ± 4
4	18	45	101	520 ± 30
5	15	45	105	560 ± 20
6	12	45	110	610 ± 20
7	8.0	45	131	698 ± 8
8	9.6	45	135	710 ± 8
9	6.8	45	138	717 ± 7
10	7.4	45	143	729 ± 7
11	85	60	85	340 ± 13
12	94	60	115	400 ± 20
13	64	60	132	520 ± 14
14	30	60	152	614 ± 10
15	37	60	161	642 ± 7.4
16	24	60	166	655 ± 7.3
17	24	60	178	684 ± 6
18	270	75	125	342 ± 8
19	220	75	135	393 ± 9
20	120	75	149	460 ± 30
21	110	75	169	541 ± 8
22	75	75	176	564 ± 7
23	79	75	190	602 ± 7

<sup>a</sup> Conditions are listed along with the rate data. Experimental procedures are described in the text. Errors in the measured rate constants are estimated to be less than 10% on the basis of uncertainties in the concentration of *N*-ethylmaleimide, errors in the spectroscopic technique, and adsorption of 9-hydroxyanthracene to the reactor walls. Density was calculated using the EOS recommended by Span and Wagner,<sup>47</sup> and the error was estimated from the accuracy of pressure/temperature measurements.

The disappearance of diene was monitored at 380 nm for at least 2 half-lives. Assumed first-order plots were linear, and the uncertainties in the slopes were less than 1%. The bimolecular rate constant was recovered by dividing the pseudo-first-order slopes by the known concentration of *N*-ethylmaleimide. For the water measurements, concentrated solutions of 9-hydroxymethylanthracene in acetonitrile were used to deliver the diene. The resulting concentration of acetonitrile was less than 1% on a mole basis.

## Results

**Measured Rate Constants.** All 23 measured rate constants (which are referred to as  $k_c$  when reported in molar units) for reaction I in scCO<sub>2</sub> are listed in Table 1 together with the conditions of the measurement (pressure/density, temperature, initial concentrations). Errors in the density were predicted using an EOS for pure carbon dioxide<sup>47</sup> and the ranges of the pressure/temperature based on the known uncertainties of the measurement. At 45 °C and 90 bar, the reaction rate measured in scCO<sub>2</sub> is nearly 25× faster than that measured in acetonitrile<sup>37,43</sup> (also measured at 45 °C but at atmospheric pressure), quite a remarkable acceleration considering that the Diels–Alder reaction between cyclopentadiene and ethyl acrylate is slower in scCO<sub>2</sub> than conventional solvents such as methylene chloride, tetrahydrofuran, and hexane.<sup>14</sup> The dramatic acceleration demonstrates that using scCO<sub>2</sub> as a reaction solvent can have significant technological advantages in addition to its well-known positive environmental attributes.

Figure 4 contains a plot of  $k_c$  as a function of pressure. At a given temperature, the rate constants clearly decrease with pressure. To our knowledge the only published report of decreasing rate constants with increasing pressure/density for a Diels–Alder reaction in scCO<sub>2</sub> is that of Thompson et al.<sup>8</sup> These authors studied the hetero-Diels–Alder reaction of anthracene

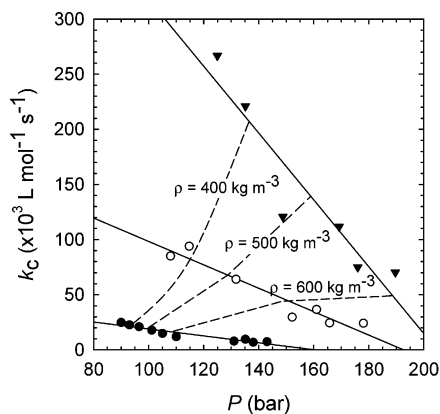


**Figure 4.** Values of  $k_c$  measured for reaction I in  $\text{scCO}_2$  plotted as a function of pressure at (●) 45 °C, (○) 60 °C, and (▼) 75 °C. Numerical values of  $k_c$  are listed in Table 1. Solid lines are the best fits for the data and have no physical basis. Dashed lines represent contours of constant fluid density, calculated assuming that the mixture is pure carbon dioxide.

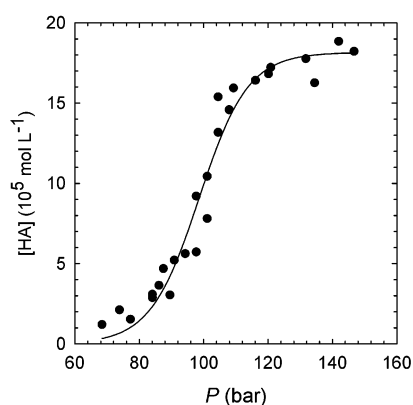
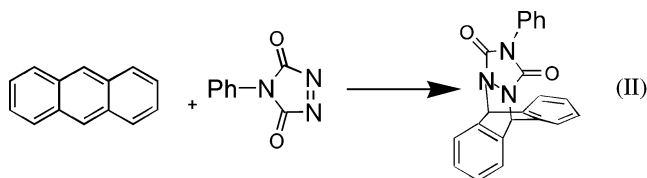


**Figure 5.** Solubility of 9-hydroxymethylanthracene, [HA], in  $\text{scCO}_2$  at 45 °C plotted as a function of pressure. The solid line is intended to guide the eye, and no physical basis is intended.

and 4-phenyl-1,2,4-triazoline-3,5-dione at 40 °C (reaction II). Reaction II is quite similar to the model reaction I chosen for this study. Therefore, it is not entirely surprising that the two reactions exhibit similar behavior with pressure/density. The similarity between reactions I and II is pursued further in the Discussion.



At a constant temperature, the rate constants are roughly linear functions of pressure ( $R^2 \geq 0.90$ ) for the entire data set. The data do not indicate any anomalous behavior near the critical pressure of carbon dioxide, and the magnitudes of the slopes of  $k_c$  versus either pressure or density (which is not shown) increase smoothly with temperature above the critical point of pure carbon dioxide.

**Solubilities of 9-Hydroxymethylanthracene in  $\text{scCO}_2$ .** The measured solubilities of 9-hydroxymethylanthracene in  $\text{scCO}_2$  at 45 °C are plotted in Figure 5. The solubility increases from  $1.2 \times 10^{-5}$  to  $1.9 \times 10^{-4}$  mol  $\text{L}^{-1}$  for the pressure range between 70 and 150 bar. There is a sharp increase in the

solubility near 75 bar related to the significant density increase in the vicinity of the critical point. The solubility of 9-hydroxymethylanthracene follows a trend similar to that observed for anthracene.<sup>48</sup> The parent compound is roughly 10× less soluble in  $\text{scCO}_2$  than 9-hydroxymethylanthracene, which can be attributed to two factors: (1) weak specific interactions between the methanol group of 9-hydroxymethylanthracene and carbon dioxide and (2) higher vapor pressure of 9-hydroxymethylanthracene relative to anthracene, due to less efficient packing in the solid state.

## Discussion

The rate of the Diels–Alder reaction of 9-hydroxymethylanthracene and *N*-ethylmaleimide is accelerated in  $\text{scCO}_2$  relative to conventional solvents. Furthermore, at all temperatures for which data are available, the rate constants decrease with increasing pressure/density. We propose that the solvophobic effect is the physical cause for both of these observations. A solvophobic mechanism is consistent with the experimental rate and solubility measurements and is further supported by activation volume estimates, comparison to reaction rates in conventional solvents, and empirical correlations.

**Effect of Pressure on Reaction Rates.** To interpret the pressure effect on kinetic data for reactions conducted in supercritical fluids, many researchers invoke transition-state theory. Within this context, the pressure dependence of the rate constant is given by

$$\left(\frac{\partial \ln(k_x)}{\partial P}\right)_{T,x} = -\frac{\Delta V^\ddagger}{RT} \quad (1)$$

where  $k_x$  is the bimolecular rate constant expressed in mole fraction units,  $T$  and  $P$  are the system absolute temperature and pressure,  $R$  is the universal gas constant,  $x$  is the concentration in mole fraction units, and  $\Delta V^\ddagger$  is the apparent activation volume. Sometimes an overbar is used in conjunction with  $\Delta V^\ddagger$  to specify that it is a partial molar quantity. The following formula is used to convert between conventional concentration units,  $k_c$ , and mole fraction concentration units  $k_x$ :

$$k_c = \frac{k_x}{(\rho/M_w)} \quad (2)$$

where  $\rho$  is the mixture fluid density (expressed as  $\text{g L}^{-1}$ ) at the temperature and pressure of the kinetic measurement and  $M_w$  is the average molecular weight of all of the species in the mixture.

The apparent activation volume is composed of two terms, one of which accounts for the formation/breaking of bonds while the other deals with changes in solvation which accompany the reaction. For structured fluids such as water or for compressible fluids such as those near their critical point,  $\Delta V^\ddagger$  may be dominated by changes in solvation volumes. Also, for reaction mechanisms which consist of multiple steps, interpretation of  $\Delta V^\ddagger$  is not straightforward and rarely provides mechanistic insights. For true elementary reactions, such as the Diels–Alder cycloaddition, molecular-level information can be obtained in principle.

(48) Bunker, C. E.; Rollins, H. W.; Gord, J. R.; Sun, Y. *J. Org. Chem.* **1997**, *62*, 7324.

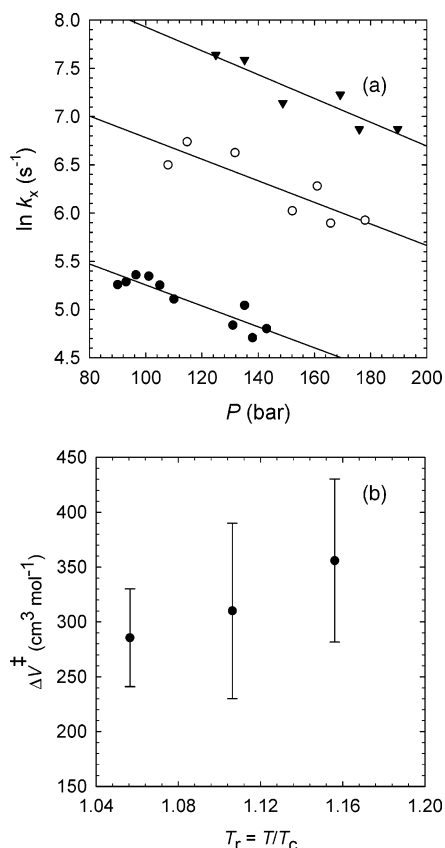


**Figure 6.** (a) Natural logarithms of  $k_x$  measured for reaction I in  $\text{scCO}_2$  plotted as a function of pressure as suggested by eq 1: ●, 45 °C; ○, 60 °C; ▼, 75 °C. Solid lines are the best fits for the data and are related to apparent values of  $\Delta V^\ddagger$ . (b)  $\Delta V^\ddagger$  determined from the slopes of the curves in Figure 6a plotted as a function of reduced temperature. Error bars are based on uncertainties in these slopes.  $\Delta V^\ddagger$  is a weak function of temperature, if it is a function of temperature at all.

Figure 6a is a plot of the natural logarithm of rate constants in mole fraction units (i.e.,  $k_x$ ) as a function of pressure at different temperatures. The slopes of these curves are essentially linear ( $R^2 > 0.80$ ), and the lines are roughly parallel. Equation 1 was used to determine apparent values of  $\Delta V^\ddagger$ , and the results are plotted as a function of reduced temperature ( $T_r = T/T_c$ ) in Figure 6b. The error bars in Figure 6b represent the uncertainties in the slopes of the best-fit lines in Figure 6a. The values of  $\Delta V^\ddagger$  for the data set are both large and positive ( $+350 \text{ cm}^3 \text{ mol}^{-1}$ ). For comparison, consideration of only the contributions from bond breaking/formation leads to estimates of  $\Delta V^\ddagger$  of roughly  $-30 \text{ cm}^3 \text{ mol}^{-1}$ . Jenner and Gacem<sup>44</sup> reported values of  $\Delta V^\ddagger$  ranging from  $-27$  to  $-36 \text{ cm}^3 \text{ mol}^{-1}$  from their studies of pressure effects on Diels–Alder reactions. Since the volume change associated with bond breaking/formation should not be strongly affected by the solvent, there must be a significant effect (roughly  $+380 \text{ cm}^3 \text{ mol}^{-1}$ ) on the apparent values of  $\Delta V^\ddagger$  measured in this study which arises from solvation.

Proximity to the critical point has only a minimal effect on  $\Delta V^\ddagger$  since there is only a weak trend in the apparent activation volume in the range of reduced temperature considered in this study (1.06–1.23). As the critical point is approached, there may be a slight increasing trend in  $\Delta V^\ddagger$  with temperature, but uncertainties in the estimated values of  $\Delta V^\ddagger$  are as large as the total change itself. This observation suggests that critical phenomena such as reactant clustering (either solute–solvent

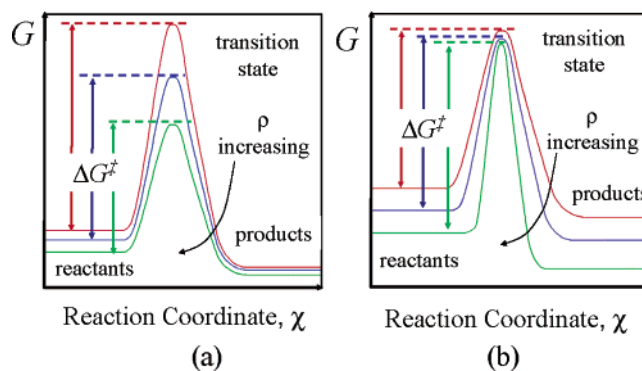


**Figure 7.** Free energy sketches for reaction coordinates representing two different responses to density. (a) shows preferential solvation of the transition state as density increases, leading to a net decrease in  $\Delta G^\ddagger$  with increasing density. In (b) the reactants are preferentially solvated by increased density, leading to a net increase in  $\Delta G^\ddagger$  as density increases. Diels–Alder reactions of highly  $\text{scCO}_2$  soluble reactants are represented by (a), while (b) depicts the situation for sparingly  $\text{scCO}_2$  soluble reactants, such as those selected for this study.

or solute–solvent) arising from density fluctuations invoked by previous researchers<sup>49</sup> do not play a role in the observed chemical kinetics.

Several researchers<sup>8,9,20,21</sup> have used cubic EOSs to predict the partial molar volumes in eq 1, thereby relating measured rate constants (or at least trends in rate constants) to pressure. The EOS approach usually requires estimates of  $T_c$ ,  $P_c$ , the accentricity factor ( $\omega$ ), and the binary interaction parameter ( $k_{ij}$ ).<sup>50</sup> Since thermodynamic parameters are well defined only for stable species, it is frequently assumed that the product and transition state are thermodynamically equivalent. Furthermore, interaction parameters are generally assumed to be zero<sup>8,9,20</sup> or small<sup>21</sup> compared to unity. Naturally these assumptions introduce some uncertainty. For instance, Thompson et al.<sup>8</sup> found that changing the estimated critical temperature of the product (and thus transition state) by 20% led to entirely different signs in EOS predictions of  $\Delta V^\ddagger$ . This casts suspicion on the use of eq 1 to provide physical insight or as a predictive tool.

We propose a different physical picture to describe the relationship between rate constants and pressure/density in  $\text{scCO}_2$ . Instead of the activation volume approach, we employ a theory of preferential solvation to explain trends in reaction rate with pressure. Figure 7 is a schematic of the physical situation in terms of changes in free energy as a function of reaction coordinate,  $\chi$ . In both panels, there is an increase in free energy upon combination of the reagents to form the transition state depicting the activation free energy for the chemical reaction,  $\Delta G^\ddagger$ . Likewise in both panels, increasing fluid density decreases the free energy of the reagents, transition state, and product. The difference between the panels is the influence of density on the barrier height,  $\Delta G^\ddagger$ . In Figure 7a, the *transition state* is preferentially solvated relative to the *reactants*; therefore,  $\Delta G^\ddagger$  is a decreasing function of density. The reaction rate constant is related to  $\Delta G^\ddagger$  by the Eyring equation:

(49) Ellington, J. B.; Brennecke, J. F. *J. Chem. Soc., Chem. Commun.* **1993**, 1094.

(50) Tester, J. W.; Modell, M. *Thermodynamics and its Applications*, 3rd ed.; Prentice Hall PTR: Upper Saddle River, NJ, 1997; Chapter 9.

$$k_c = \frac{k_B T}{h} \exp(-\Delta G^\ddagger/RT) \quad (3)$$

where  $k_B$  is Boltzmann's constant ( $1.38 \times 10^{-23} \text{ J K}^{-1}$ ) and  $h$  is Planck's constant ( $6.6261 \times 10^{-34} \text{ J s}$ ). Equation 3 predicts that a decrease in  $\Delta G^\ddagger$  leads to an increase in  $k_c$ . Since reactions in  $\text{scCO}_2$  are typically accelerated by increased pressure/density, Figure 7a describes the physical situation most frequently observed in experimental measurements of rate constants in supercritical fluids. Figure 7b depicts the opposite relationship between density and reaction rate in which the *reactants* are solvated preferentially relative to the *transition state*. The free energy curves in Figure 7b show  $\Delta G^\ddagger$  as an increasing function of density, which, according to eq 3, predicts that the rate constants will decrease as pressure/density increases. This is the behavior reported in this study and that of Thompson et al.<sup>8</sup>

Reported kinetic rate measurements of Diels–Alder reactions in  $\text{scCO}_2$  can be divided into two groups corresponding to panels a and b, respectively, of Figure 7. The first, more populated group corresponds to Diels–Alder reactions in which the reactants are rather soluble in  $\text{scCO}_2$ . Many of the most common dienes (isoprene, cyclopentadiene) and dienophiles (methyl acrylate, ethyl acrylate, maleic anhydride) in this group are either essentially miscible with  $\text{scCO}_2$  or at least reasonably soluble. Of the reagents commonly used in this group of Diels–Alder reactions, maleic anhydride is the least soluble in  $\text{scCO}_2$  with a measured solubility estimated<sup>7</sup> as 0.2 mol % at 60 °C and 100 bar. This contrasts with the second group, which includes this data set, in which the solubilities of the dienes are much lower, on the order of  $1 \times 10^{-3}$  mol %, or less.

Consideration of transition-state theory provides a more physical interpretation of the observed rate phenomena and their relationship to reagent solubility. In this context,  $k_c$  is expressed as

$$k_c = \kappa \frac{k_B T}{h} K_C^\ddagger \quad (4)$$

where  $\kappa$  is the transmission coefficient ( $0 \leq \kappa \leq 1$ ) and  $K_C^\ddagger$  is the concentration-based equilibrium constant for the reaction between the reactants and transition state, which, for an elementary reaction such as the Diels–Alder cycloaddition, is defined as

$$K_C^\ddagger = \frac{C_{A-B}^\ddagger}{C_A C_B} \quad (5)$$

where  $C_A$  and  $C_B$  are the molar concentrations of the reactants and  $C_{A-B}^\ddagger$  is the “concentration” of the idealized transition state. Following a standard thermodynamic procedure, most of which can be found in the literature<sup>14,51,52</sup> and is further documented in the Supporting Information, eq 5 can be written as

$$k_c = \kappa \frac{k_B T}{h} \exp\left(\frac{-\Delta G^{\ddagger,0}}{RT}\right) \frac{1}{M_W} \frac{K_{x,\text{sat}}^\ddagger}{K_{x,\text{id}}^\ddagger} \quad (6)$$

where  $\Delta G^{\ddagger,0}$  is the change in partial molar Gibbs free energy

between reactants and transition state when all species are in their respective standard states,  $K_{x,\text{id}}^\ddagger$  is the continued product of the ideal solution mole fraction solubilities, and  $K_{x,\text{sat}}^\ddagger$  is the continued product of the actual saturation mole fraction solubilities. By definition  $K_{x,\text{id}}^\ddagger$  is not a function of pressure,<sup>53</sup> and neither is  $\Delta G^{\ddagger,0}$  provided that the reference states are defined at a fixed pressure. Therefore, assuming that  $\kappa$  is at most a weak function of pressure, the majority of the pressure dependence in eq 6 is due to  $K_{x,\text{sat}}^\ddagger$ .

Equation 6 allows interpretation of Figure 7a,b in terms of solubility or solvation. Increases in fluid density have little effect on the solubility of dienes, which are essentially miscible with  $\text{scCO}_2$ . For Diels–Alder reactions of these dienes, the transition state is much less solvated in  $\text{scCO}_2$ . This is rationalized by the fact that, in thermodynamic terms, the primary difference between the reactants and the transition state is the molecular size. It is well-known that, as the molecular size of compounds increases, their solubility in  $\text{scCO}_2$  decreases. This is particularly true when molecular size is increased without introduction of new functional groups. The examples of benzene (which is essentially miscible with  $\text{scCO}_2$ ), naphthalene (which has a characteristic solubility of approximately 5 wt % in  $\text{scCO}_2$  at 35 °C and 150 bar<sup>54</sup>), and anthracene (the solubility of which is less than  $5 \times 10^{-3}$  wt % at 35 °C and 150 bar<sup>48</sup>) are illustrative. Increasing the density does not substantially increase the solubility of compounds already miscible with  $\text{scCO}_2$ , such as benzene or typical Diels–Alder reactants. Unlike the reactants, the solvation of the large transition state, which contains no functional groups not present in the reactants, increases significantly with fluid density. Thus,  $K_{x,\text{sat}}^\ddagger$  increases with pressure, which leads to an increase in  $k_c$ .

The situation is reversed for dienes which are sparingly soluble in  $\text{scCO}_2$  such as anthracene and 9-hydroxymethylanthracene. The solubilities of these reactants increase sharply with density as depicted for 9-hydroxymethylanthracene in Figure 5. The solvation of the transition state most likely also increases with fluid density, but we hypothesize that the effect is less significant than for the reactants. Therefore, for these reactions,  $K_{x,\text{sat}}^\ddagger$  decreases with pressure, leading to a decrease in  $k_c$ . This hypothesis is supported by the fact that a fraction of the insoluble surface area of the diene becomes inaccessible to the solvent during the course of the reaction. Figure 8 contains optimized geometries of the reactants and transition state for reaction I as calculated by Gaussian 98 (B3LYP/6-31Gd) and depicts the solvent-inaccessible surface area of the transition state. Due to the reduced requirement for solvent interactions with the transition state, it is preferentially solubilized as density is decreased. This is a solvophobic effect analogous to those reported in water<sup>37–42</sup> and fluorocarbon solvents.<sup>43–45</sup> The large, positive values of  $\Delta V^\ddagger$  observed for our rate data are related to changes in the preferential solvation of the transition state relative to the reactants as pressure decreases rather than true changes in molecular volumes (of either the reactants/transition state or solvent). Critical phenomena cannot explain the observed

(51) Clifford, A. Physical Properties as Related to Chemical Reactions. In *Chemical Synthesis Using Supercritical Fluids*; Jessop, P. G., Leitner, W., Eds.; Wiley-VCH: New York, 1999; Chapter 3.

(52) Weinstein, R. W. Ph.D. Thesis, Massachusetts Institute of Technology, Cambridge, MA, 1998.

(53) Prausnitz, J. M.; Lichtenthaler, R. N.; Gomes de Azevedo, E. *Molecular Thermodynamics of Fluid-Phase Equilibria*, 3rd ed.; Prentice Hall PTR: Upper Saddle River, NJ, 1999; Chapters 6 and 11.

(54) Modell, M.; de Filippi, R. P.; Krukoni, V. J. *Regeneration of Activated Carbon with Supercritical Carbon Dioxide*, ACS Annual Meeting, Miami, FL, 1978; American Chemical Society: Washington, DC, 1978.

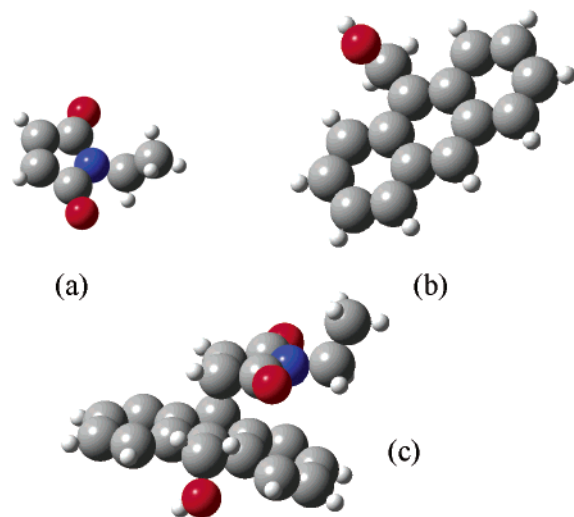


**Figure 8.** Optimized geometries of (a) *N*-ethylmaleimide, (b) 9-hydroxymethylantracene, and (c) their Diels–Alder cycloaddition transition state. All geometries were optimized using Gaussian 98 (B3LYP/6-31Gd).

pressure/density behavior since  $\Delta V^\ddagger$  is only a weak function of reduced temperature. In any event, solute/solute and solute/solvent clustering should be negligible for  $T_r > 1.1$ .<sup>55</sup>

**Solvophobic Interactions and Acceleration of Diels–Alder Reactions.** The Diels–Alder reaction between 9-hydroxymethylantracene and *N*-ethylmaleimide has been studied previously in conventional solvents.<sup>37,43</sup> These studies have clearly implicated the accelerative roles of hydrogen-bonding and solvophobic interactions. Most convincingly, Myers and Kumar<sup>43</sup> demonstrated that the bimolecular rate constants for this reaction measured at 45 °C in a range of solvents were inversely related to the solubilities of the diene in the same solvent, with significant deviations observed only for reactions conducted in solvents capable of hydrogen bond donation (e.g., water and trifluoroethanol). Table 2 lists available experimental measurements of the rate constant of reaction I, along with the solubility of 9-hydroxymethylantracene, and  $-\Delta\Delta G^\ddagger$ , which is the change in the activation free energy relative to that observed in acetonitrile calculated using eq 3. Duplicate values of  $k_c$ , when available, agree to within experimental error with the exception of those obtained in water. In this study, 1 mol % acetonitrile was used as a delivery solvent for rate studies in water. Most likely, this small amount of acetonitrile acted as a cosolvent, reducing the solvophobic effect and decelerating the reaction rate.

Values of  $-\Delta\Delta G^\ddagger$  reported in Table 2 range from zero (for acetonitrile, by definition) to roughly 6 kJ mol<sup>-1</sup> (for water). Values of  $-\Delta\Delta G^\ddagger$  for scCO<sub>2</sub> bridge the gap between fluorocarbon and hydrocarbon solvents. Changes in fluid density in the supercritical solvent are similar to changes in the chemical identity of incompressible solvents. Increasing the scCO<sub>2</sub> fluid density from 340 to 730 kg m<sup>-3</sup> is roughly equivalent to changing the solvent from perfluoro-*n*-butyl ether to 1-butanol. Just as in conventional solvents, the slowest rate constants are observed in scCO<sub>2</sub> under conditions at which 9-hydroxymethylantracene is most soluble. Naturally, the accelerative effect of scCO<sub>2</sub> is less than that of water since carbon dioxide lacks the capacity to form hydrogen bonds. Nonetheless, solvophobic reduction of  $\Delta G^\ddagger$  in scCO<sub>2</sub> is significant.

**Table 2.** Rate Constants,  $k_c$ , for the Diels–Alder Reaction of 9-Hydroxymethylantracene and *N*-Ethylmaleimide at 45 °C in Hydrocarbon Solvents, Fluorocarbon Solvents, Water, and scCO<sub>2</sub><sup>a</sup>

solvent	$k_c$ (10 <sup>5</sup> L mol <sup>-1</sup> s <sup>-1</sup> )	$-\Delta\Delta G^\ddagger$ <sup>b</sup> (kJ mol <sup>-1</sup> )	solubility (10 <sup>3</sup> mol L <sup>-1</sup> )	source
Supercritical Fluid Solvents				
scCO <sub>2</sub> , $\rho =$ 340 g L <sup>-1</sup>	2480 ± 250	4.0	0.03	this work
scCO <sub>2</sub> , $\rho =$ 560 g L <sup>-1</sup>	1490 ± 150	3.0	0.13	this work
scCO <sub>2</sub> , $\rho =$ 730 g L <sup>-1</sup>	740 ± 100	1.8	0.18	this work
Hydrocarbon Solvents				
<i>n</i> -hexane	776 ± 80	2.3	1.24	43
isooctane	796 ± 71	2.3	na <sup>d</sup>	37
di- <i>n</i> -butyl ether	245 ± 16	0.9	20.9	43
acetonitrile	108 ± 10	0.0	29.5	43
	107 ± 8			37
	100 ± 6			this work
methanol	337 ± 60	1.3	29.9	43
	344 ± 25			37
1-butanol	666 ± 23	2.1	na <sup>d</sup>	37
Fluorocarbon Solvents				
perfluorohexane	5345 ± 308	4.5	>0.005	43
perfluoro-2- <i>n</i> -butyl ether <sup>c</sup>	4562 ± 404	4.3	>0.005	43
perfluorobenzene	152 ± 26	0.4	11.2	43
trifluoroethanol	841 ± 114	2.4	18.1	43
water	22300 ± 720	6.1 <sup>e</sup>	0.027	43
	22600 ± 700			37
	18400 ± 300			this work

<sup>a</sup> Solubilities of 9-hydroxymethylantracene at 45 °C are also listed, where available.  $\Delta\Delta G^\ddagger$  is the change in activation free energy relative to that in acetonitrile. <sup>b</sup> Relative to the average value measured for acetonitrile, calculated using eq 3. <sup>c</sup> Also referred to by its trade name FC-75. <sup>d</sup> Solubility measurement not available. <sup>e</sup> Average value of  $-\Delta\Delta G^\ddagger$  based on the data of Rideout and Breslow<sup>37</sup> and Myers and Kumar.<sup>43</sup>

Understanding the solvophobic acceleration of Diels–Alder reactions in scCO<sub>2</sub> provides a tool for selection of model reactions to conduct in supercritical fluids. Typically, reagent selection is based on solubility in scCO<sub>2</sub>. Solvophobic acceleration offers a second criterion for the choice of reagents. The analogy with fluorinated solvents (which are more accessible experimentally than scCO<sub>2</sub>) might also be exploited in the future.

Of course, scale-up of reactions involving sparingly soluble species may be prohibitive just as has been the case for utilizing water as a solvent for Diels–Alder reactions and other syntheses. It might be possible to follow the strategy of Greico et al.,<sup>56</sup> who demonstrated that addition of solvophilic functionalities far from the reactive portion of the molecule increase water solubility while maintaining most of the beneficial effects of water on reactivity. In fact, the 10-fold increase of the solubility of 9-hydroxymethylantracene compared to anthracene cited in this study is a prime example of this strategy.

**Engineering Correlations Based on the Arrhenius Equation.** Correlations for data sets of experimental rate constants as functions of operating conditions (temperature, pressure/density) are quite valuable in commercial applications. The Arrhenius equation is the typical starting point for correlating rate data:

$$k_c = A \exp(-E_A/RT) \quad (7)$$

where  $A$  is the preexponential factor and  $E_A$  is the apparent

(55) Tucker, S. *Chem. Rev.* **1999**, *99*, 391.

(56) Grieco, P. A.; Yoshida, K.; He, Z. *Tetrahedron Lett.* **1984**, *25*, 5715.

**Table 3.** Empirically Fit Arrhenius Parameters and Estimated Errors for Reaction I in Water and Acetonitrile

solvent	$\ln A$ ( $\text{L mol}^{-1} \text{s}^{-1}$ )	$E_A$ ( $\text{kJ mol}^{-1}$ )
water	$16.86 \pm 0.03$	$51.6 \pm 2.3$
acetonitrile	$12.72 \pm 0.03$	$52.0 \pm 2.3$

activation energy. The Eyring equation is frequently written in ad hoc fashion analogous to eq 7 by substituting the relationship

$$\Delta G^\ddagger = \Delta H^\ddagger - T\Delta S^\ddagger \quad (8)$$

into eq 3, yielding the following equation:

$$k_c = \frac{k_B T}{h} \exp(\Delta S^\ddagger/R) \exp(-\Delta H^\ddagger/RT) \quad (9)$$

Even though the  $\Delta H^\ddagger$  and  $T\Delta S^\ddagger$  terms contain global information, they can be interpreted using the Arrhenius model. The entropic term is related to  $A$  in eq 7, and the enthalpic term is related to  $E_A$ . For well-defined reactions such as the bimolecular Diels–Alder cycloaddition, the physical significance of these two terms can sometimes be retained. In their studies of Diels–Alder reaction kinetics in water and 2-propanol, Engberts and co-workers<sup>57</sup> determined that the entropic and enthalpic contributions to  $\Delta G^\ddagger$  were roughly equal. In practice,  $A$  and  $E_A$  are correlated so that rate data may not yield unambiguous values of  $\Delta H^\ddagger$  and  $T\Delta S^\ddagger$ .

As written, eqs 3 and 7 cannot describe the data set presented in Table 1 since the Arrhenius and Eyring equations have no explicit dependence on pressure/density. In an earlier study,<sup>14</sup> we introduced a modified form of eq 7 in which  $A$  was a linear function of density

$$k_c = (\alpha\rho + \beta) \exp(-E_A/RT) \quad (10)$$

to fit rate data for the reaction of cyclopentadiene and ethyl acrylate. A similar approach was considered for our data set, but some caution was exercised. Equation 10 is nonlinear, necessitating a nonlinear regression of the parameters  $\alpha$ ,  $\beta$ , and  $E_A$ . Finding optimum parameters by nonlinear regression is complicated by the potential existence of many local minima, and there is no guarantee that the global minimum corresponds to physical values of the parameters. To constrain the allowable ranges of  $\alpha$ ,  $\beta$ , and  $E_A$  to physical values, Arrhenius parameters for reaction I were obtained in water and acetonitrile. The values obtained in these solvents are listed in Table 3. Water and acetonitrile were selected to bracket the rate constant data reported in Table 2. Note that the two values of  $E_A$  are identical, within the limits of experimental uncertainty. Values of  $A$ , however, differ by nearly 2 orders of magnitude. These results suggest that it is reasonable to use eq 10 to describe the data set obtained in  $\text{scCO}_2$ , constraining the range of values of  $E_A$  and  $A$  for interpreting rate data in the supercritical medium.

Figure 9 is a plot of the measured rate constants ( $k_c$ ) for reaction I as a function of density. The solid lines represent the predictions of eq 10 using best fit values for  $\alpha$  and  $\beta$ , with  $E_A$  set equal to 52  $\text{kJ mol}^{-1}$ . On the basis of these fitted parameters, the natural logarithm of  $A$  varies between 14.5 and 16.4 (when  $A$  is expressed as  $\text{L mol}^{-1} \text{s}^{-1}$ ), which is within the limits

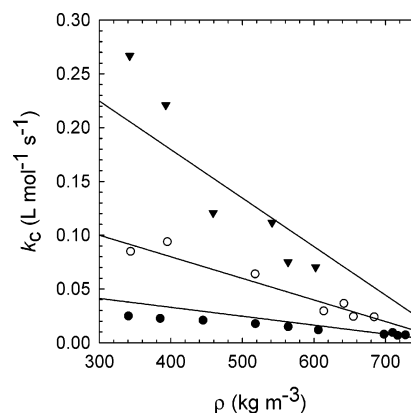


**Figure 9.**  $k_c$  measured for reaction I in  $\text{scCO}_2$  plotted as a function of density: ●, 45 °C; ○, 60 °C; ▼, 75 °C. Solid lines are based on regression of  $\alpha$  and  $\beta$  in eq 10.  $E_A$  was set equal to 52  $\text{kJ mol}^{-1}$  on the basis of its value in acetonitrile and water, and  $\ln A$  varied linearly from 14.5 (at 730  $\text{kg cm}^{-3}$ ) to 16.4 (at 340  $\text{kg cm}^{-3}$ ).

suggested by the data in Table 3. Not only does eq 10 provide a good correlation for the available data, it uses physically realistic values of the various parameters. This further supports the theory that chemical reactivity in supercritical fluids is analogous to that in incompressible solvents, provided that changes in the relative solubilities of reactants and transition states are properly accounted for. We also note that defining both  $A$  and  $E_A$  as linear functions of density (but still constraining their range of allowable values on the basis of the parameters in Table 3) introduces some curvature to predictions of  $k_c$ , which might capture trends better, especially at 75 °C. Quantitatively, to any reasonable level of statistical confidence, the two models are identical.

## Conclusions and Recommendations

The Diels–Alder reaction of dienophile *N*-ethylmaleimide with 9-hydroxymethylanthracene proceeds at rates in supercritical carbon dioxide that are much faster than in traditional organic solvents such as acetonitrile, methanol, etc. On the basis of the low solubility of 9-hydroxymethylanthracene, we infer a solvophobic mechanism consistent with that proposed for acceleration of this reaction in conventional solvents. Strong, negative pressure and density dependencies of the rate constant were observed, consistent with a solvophobic mechanism driven by the positive relationship between fluid density and solute solubility. The apparent activation volumes are both large and positive (+350  $\text{cm}^3 \text{mol}^{-1}$ ), and only a weak function of reduced temperature, ruling out the influence of clustering phenomena (solute/solvent or solute/solute) as the cause of the observed accelerations. Instead, the large activation volumes can be attributed to changes in the solubility of the reagents relative to that of the transition state with increasing density. Our results suggest an analogy between supercritical carbon dioxide and fluorinated solvents which may be useful for selecting model reactions and interpreting solvent effects.

Future work will be conducted to further understand this solvophobic acceleration so that the results uncovered by this investigation might be applied to a wider range of organic reactions. Studies will focus on (1) determination of specific molecular structures which are expected to interact solvophobically in  $\text{scCO}_2$ , (2) further quantification of the solvophobic effect, particularly in the presence of hydrogen-bond-donating

(57) Blokzijl, W.; Blandamer, M. J.; Engberts, J. B. F. *N. J. Am. Chem. Soc.* **1991**, *113*, 4241.

cosolvents, and (3) development of computational techniques integrating methods from density functional theory and molecular simulation to further molecular-level understanding of reactivity in scCO<sub>2</sub>.

**Acknowledgment.** We gratefully thank the U.S. Environmental Protection Agency Technology for a Sustainable Environment Program (Agreement No. R 826738-01-0) and the Cambridge University-Massachusetts Institute of Technology (MIT) Institute (CMI) for providing partial support for this research. J.Q. thanks the Knut and Alice Wallenberg Foundation (Sweden) for support as a Postdoctoral Fellow in Environment and Sustainability. M.T.T. received fellowship support from the Martin Family Foundation. C.J.R. was supported by MIT's Undergraduate Research Opportunity Program. Members of the Supercritical Fluids Group at MIT developed some aspects of the experimental techniques. T. A. Hatton graciously provided access to the spectrophotometer used for studying reaction

kinetics at atmospheric pressure. M.T.T. enjoyed fruitful discussions with William Green, Sumathy Raman, and James Taylor of the Chemical Engineering Department at MIT. Josh Dunetz, Jason Diffendal, and Rick Danheiser of the Chemistry Department at MIT, Melanie Tsang, Catherine Smith, and Andrew Holmes of the Chemistry Department at Cambridge University, and Liz Gron of the Chemistry Department at Hendrix College shared their extensive knowledge of synthetic chemistry. We also thank Federico Pacheco (now at Stanford University) and Laura Shimmin for their assistance with some of the experimental procedures.

**Supporting Information Available:** More details regarding the MS/MS analytical technique and a detailed derivation of eq 6 (PDF). This material is available free of charge via the Internet at <http://pubs.acs.org>.

JA030620A